

Globular clusters as laboratories for stellar evolution

Márcio Catelan,¹ Aldo A. R. Valcarce,¹ and Allen V. Sweigart²

¹Pontificia Universidad Católica de Chile, Departamento de Astronomía y Astrofísica,
Av. Vicuña Mackenna 4860, 782-0436 Macul, Santiago, Chile
email: [mcatelan, avalcarc]@astro.puc.cl

²NASA Goddard Space Flight Center, Exploration of the Universe Division, Code 667,
Greenbelt, MD 20771, USA
email: allen.v.sweigart@nasa.gov

Abstract. Globular clusters have long been considered the closest approximation to a physicist's laboratory in astrophysics, and as such a near-ideal laboratory for (low-mass) stellar evolution. However, recent observations have cast a shadow on this long-standing paradigm, suggesting the presence of multiple populations with widely different abundance patterns, and—crucially—with widely different helium abundances as well. In this review we discuss which features of the Hertzsprung–Russell diagram may be used as helium-abundance indicators, and present an overview of available constraints on the helium abundance in globular clusters.

Keywords. Hertzsprung–Russell diagram, stars: abundances, stars: evolution, stars: Population II, globular clusters: general

1. Introduction

In the words of Moehler (2001), “globular clusters [GCs] are the closest approximation to a physicist's laboratory in astrophysics.” Not only do these spheroidal stellar agglomerations contain up to several million stars, all at the same distance from us, but their stars have also been thought to have all been born at the same instant, from a cloud with homogeneous chemical composition. According to this canonical paradigm, GCs represent the best examples of a simple stellar population. As a result, GCs have been used extensively to place constraints on key ingredients of canonical stellar evolution models, such as the mixing-length parameter of convective energy transport theory (e.g., Palmieri *et al.* 2002; Ferraro *et al.* 2006). In addition, GC studies have played an important role in the field of particle physics, with measured color–magnitude–diagram (CMD) properties being used to place some of the strongest constraints available on several dark-matter candidates and other particle-physics parameters that play a key role in the physics beyond the so-called ‘standard model’ of particle physics, including, e.g., the neutrino magnetic moment, the mass of the axion and the cross sections of weakly interacting massive particles (e.g., Raffelt 1996, 2000, 2008; and references therein).

However, recent observations suggest that GCs may not play as reliable a role as astrophysical laboratories as previously believed. For one, large variations in some light-element abundances, particularly O, Na, Al and Mg (but, importantly, not in the iron-peak or other α -capture elements), have been found in virtually all GCs for which suitable spectroscopic data have been obtained (e.g., Carretta *et al.* 2009; and references therein), unlike what is seen among metal-poor field stars (Gratton *et al.* 2000). For another, recent *Hubble Space Telescope* observations (e.g., Piotto 2009; and references therein) have revealed the presence of multiple stellar populations in at least some of the more massive GCs in our Galaxy, including multimodal main sequences (MSs) and subgiant

branches (SGBs), possibly connected with multimodal horizontal branches (HBs), the latter having been known since much earlier (see Catelan 2008 for a recent review).

While at least some GC CMDs still reveal exquisitely tight sequences down to the bottom of the MS, with no evidence of multiple populations (or even for sizeable samples of binary stars; Davis *et al.* 2008), the fact that several GCs show split sequences strongly suggests that GCs do not all represent the simple stellar populations that they were once thought to. Instead, they appear to be chemically complex entities whose stars did not form all at the same time, undergoing instead several bursts of star formation which progressively contaminate the medium before the formation of the next stellar generation in the cluster.

Of particular importance, in this regard, is the possibility that each stellar generation may increase the helium content, Y , of the medium before the next generation forms. Helium is the second most abundant element in the Universe, and as such, changes in Y may dramatically change the stellar evolutionary paths and associated timescales. In this sense, while helium enrichment is a consistent prediction of different scenarios for the abundance variations that are seen in GCs, the amount of He enhancement differs markedly from one model to the next (e.g., Marcolini *et al.* 2009). Importantly, while the observed MS splits in some GCs indicate very large levels of He enrichment, with the He abundance in the most extreme populations reaching values as high as about 40% by mass (Norris 2004; D'Antona *et al.* 2005; Piotto *et al.* 2005, 2007), it is not straightforward to produce such large levels of He enrichment on the basis of available chemical-enrichment scenarios. In this sense, and given that He enhancements among GC stars have now been suggested to be the rule rather than the exception (with some GCs—those with purely blue HBs—possibly lacking first-generation, non-He-enriched stars altogether; e.g., D'Antona & Caloi 2008), it is important to check all possible signatures of He enhancement, based on the observed properties of GC stars, to constrain the He-enrichment scenario. This is a crucial task to help establish the extent to which at least some GCs may still be safely used as laboratories of low-mass stellar evolution. On the other hand, the heavily contaminated GCs will continue to play an important role, although as laboratories of the evolution (and ejecta produced by) more massive stars.

Since He-abundance measurements are only possible for hot stars, which are generally lacking in GCs, most of the available Y estimates use indirect techniques, based on their CMD properties. In this sense, in the next section we first review empirical determinations of the He abundance in GC stars and then discuss the impact of He-abundance variations among several GC observables, based on a new set of evolutionary tracks for canonical and He-enhanced compositions (Valcarce 2010), along with the results that have been obtained using some of these observables. Finally, in Section 3, we present our conclusions.

2. Helium-abundance measurements for GCs

2.1. Direct methods

Most GCs lack sufficiently hot stars for direct He-abundance measurements.† Even for those that contain sufficiently hot stars, primarily on the blue HB, the results of direct He-abundance measurements can be strongly affected by diffusion effects, which can dramatically lower the photospheric He abundance for HB stars hotter than 11 500 K (e.g., Behr 2003; Moehler *et al.* 2003).‡ Conversely, at the hot end of the HB, very high

† To be sure, a He I line is found in near-infrared spectra of cool red giants at 10 830 Å, but this is due to chromospheric emission and is thus a much better indicator of mass loss than of He abundance (e.g., Dupree *et al.* 2009; and references therein).

‡ This corresponds to the so-called 'Grundahl jump' (Grundahl *et al.* 1999).

photospheric He abundances have indeed been measured, which several authors have interpreted in terms of the ‘late-flasher’ scenario for the origin of these hot stars. In this scenario, stars that lose too much mass while on the red-giant branch (RGB) may ignite He not at the RGB tip, but rather as they evolve towards the white-dwarf region of the CMD, undergoing extensive mixing in the process. Their photospheres may thus become dramatically enriched in He, to levels that can be much higher than even the highest levels that have been suggested under the ‘primordial’ (multiple-population) scenario (e.g., Moehler *et al.* 2004, 2007; Cassisi *et al.* 2009; and references therein).

This leaves us with blue HB stars situated between the blue edge of the instability strip, at around 7200 K, and the Grundahl jump, at 11 500 K. Very recently, Villanova *et al.* (2009) carried out the first detailed spectroscopic He-abundance measurement for HB stars in this temperature range. Based on *VLT/UVES* spectra of cool blue HB stars in NGC 6752, they found that “... all our targets... have a homogeneous He content with a mean value $Y = 0.245 \pm 0.012$, compatible with the most recent measurements of the primordial He content of the Universe.” Note that NGC 6752, as a cluster whose HB is comprised solely of blue HB stars, might have been viewed as an object lacking first-generation (i.e., non-He-enriched) stars, but these new measurements show that even clusters having entirely blue HBs likely have at least some stars with primordial He.

2.2. Indirect Methods

In Figure 1, we show a comparison between two isochrones for an old (12 Gyr) and metal-poor ($Z = 0.0005$) population, for two different He abundances on the zero-age MS: $Y = 0.24$ (which should be representative of the ‘first generation’ of GC stars) and $Y = 0.34$ (which is even lower than the amount of He enhancement that has been suggested for some GCs; see, e.g., Table 1 in D’Antona & Caloi 2008). These models were computed using an updated version of the Schwarzschild stellar evolution code, with updated input physics as described in Valcarce (2010). The tracks assume a solar-scaled mix (and thus $[M/H] = -1.54$ for these models), but the scaling relation of Salaris *et al.* (1993) can be straightforwardly used to apply our tracks to the α -enhanced case as well.

As can be seen from Figure 1, these isochrones reveal that not only is the MS affected by an increase in the He abundance, but so are several other key evolutionary stages in the lives of low-mass stars. This is summarized in Tables 1 (for $Y = 0.24$) and 2 (for $Y = 0.34$), where the properties of the following evolutionary stages are indicated: (i) MS, at a temperature $T_{\text{eff}} = 5000$ K (corresponding to a color $B - V \simeq 0.8$ mag), (ii) MS, at a luminosity $\log(L/L_{\odot}) = -0.5$, (iii) MS turnoff (TO) point, (iv) SGB, corresponding to a point on the isochrone that is cooler than the MS TO by $\Delta \log T_{\text{eff}} = 0.03$, (v) SGB, at a temperature $\log T_{\text{eff}} = 3.78$, (vi) base of the RGB, corresponding to a point on the isochrone that is brighter than the MS TO by $\Delta \log(L/L_{\odot}) = +0.5$, (vii) base of the RGB, at a luminosity $\log(L/L_{\odot}) = +1.0$, (viii) RGB luminosity-function ‘bump,’ (ix) RGB tip, (x) zero-age HB (ZAHB), at a temperature $\log T_{\text{eff}} = 3.85$ (which is close to the blue edge of the RR Lyrae instability strip) and (xi) asymptotic giant branch (AGB) ‘clump.’ The differences between the predicted values for the two different He abundances are given in Table 3 and the implied slopes in Table 4. In what follows, we address some of the outstanding results of this analysis (see also Salaris *et al.* 2006).

MS. An expanded view of Figure 1 around the MS and SGB regions is given in Figure 2, clearly confirming that He-enhanced models are hotter and/or less luminous than their low- Y counterparts. Indeed, detections of MS splits, as mentioned in Section 1, have so far been the main indicator of variations in the He abundance within individual GCs.

MS TO. According to our results, the MS TO of a He-enhanced population is both hotter and fainter than for low Y , as can also be seen from Figure 2.

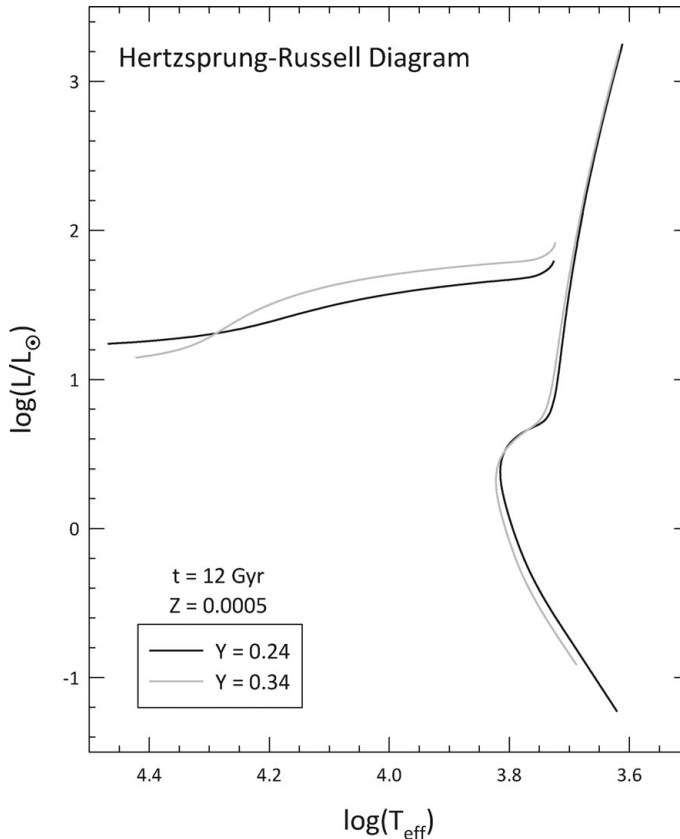


Figure 1. Isochrones for an age of 12 Gyr, metallicity $Z = 0.0005$ and two different initial helium abundances, $Y = 0.24$ (black lines) and $Y = 0.34$ (gray lines).

SGB. Our calculations reveal that the position of the SGB is *not* sensitive to Y (see also Figure 2). Differences in He abundance are thus not a viable candidate to explain the SGB splits that have been found in the literature, and changes in the abundances of other abundant species, such as the CNO elements, are accordingly also required to reproduce these splits (see also Cassisi *et al.* 2008; Salaris *et al.* 2008; Ventura *et al.* 2009).

Base of the RGB. Figure 2 shows that the base of the RGB of He-enhanced models is hotter (at a given luminosity) than their low- Y counterparts. The detected difference corresponds to $d\Delta(B - V)_{\text{RGB}}/dY \approx d\Delta(V - I)_{\text{RGB}}/dY \approx -0.35$, implying $d\Delta(B - I)_{\text{RGB}}/dY \approx -0.7$. This is not a negligible effect. As a matter of fact, Table 3 shows that the temperature split is predicted to be about half as large as the MS separation. Our calculations further reveal that such a difference in temperature, hence color, persists until the RGB tip, as can also be seen from Figures 3 and 4, although the size of the predicted split decreases progressively towards the RGB tip, where the presence of AGB stars may also complicate any empirical tests (see also Caloi & D’Antona 2005; Salaris *et al.* 2006; Pietrinferni *et al.* 2009). Still, since photometry of RGB stars is nowadays often precise to a level much better than 0.01 mag, large He enhancements might also manifest themselves as RGB splits in well-populated CMDs. On the other hand, one should also keep in mind the possibility that differences in color transformations between He-enriched and non-He-enriched GC stars might mask, at least in part, this effect (but see Girardi *et al.* 2007). Indeed, such RGB splits appear to have so far been reported

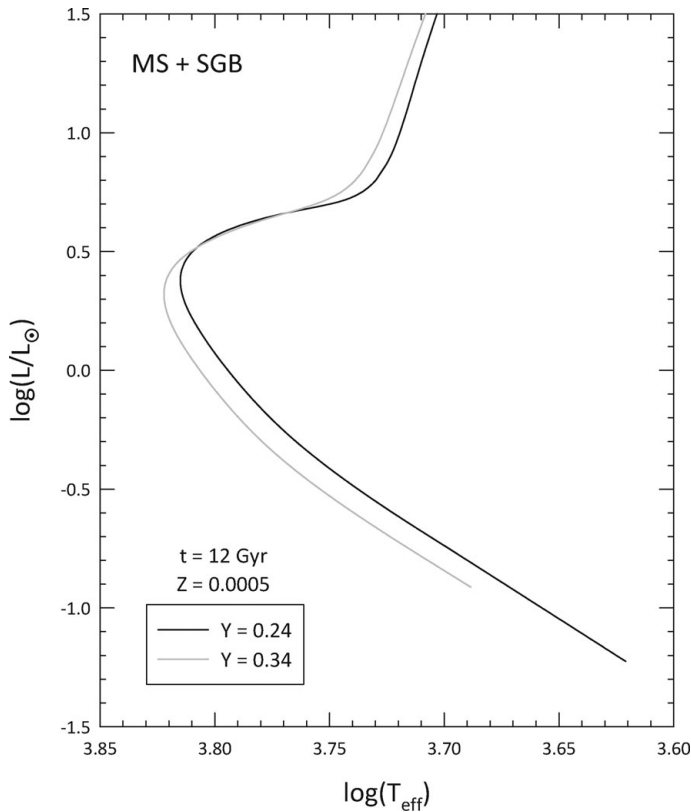


Figure 2. As Figure 1, but zooming in around the MS–SGB region.

only in the cases of M4 (NGC 6121; Marino *et al.* 2008) and NGC 1851 (Lee *et al.* 2009), and even in those cases, only using bluer passbands and the Strömgen filter system, respectively. This suggests that these RGB splits may, in reality, be due to the effect of abundance variations on the color transformations, rather than to a He enhancement proper (see also Yong *et al.* 2008, 2009), but further studies would be of much interest.

RGB bump. Our calculations confirm many previous indications that both the position and shape of the RGB bump depend sensitively on the He abundance (e.g., Salaris *et al.* 2006). This is particularly clear from Figure 3, which shows that the higher- Y models have a brighter bump than their lower- Y counterparts. Accordingly, multiple generations with widely different He abundances should also manifest themselves in the form of multiple RGB bumps. A search for these multiple bumps has been conducted for ω Cen (Sollima *et al.* 2005; F. R. Ferraro 2009, priv. comm.), with an indication that the implied range in Y is smaller than indicated by analyses of the MS splits. However, analysis of this cluster is complicated because it contains a large spread in metallicities and ages, both of which also affect the position of the RGB bump. Therefore, further analysis of this and other (monometallic) GCs would certainly prove of interest (see also Riello *et al.* 2003; Caloi & D’Antona 2005; Carretta *et al.* 2007).

Bono *et al.* (2001) carried out a comparison between the number of stars around and below the detected bump in a large and homogeneous sample of GCs and the prediction of He-enriched models. Their results, as summarized in their figure 2, again do not reveal statistically significant evidence for large He-abundance variations, except perhaps for NGC 6441 (which, however, they suggest may be an artifact of differential reddening,

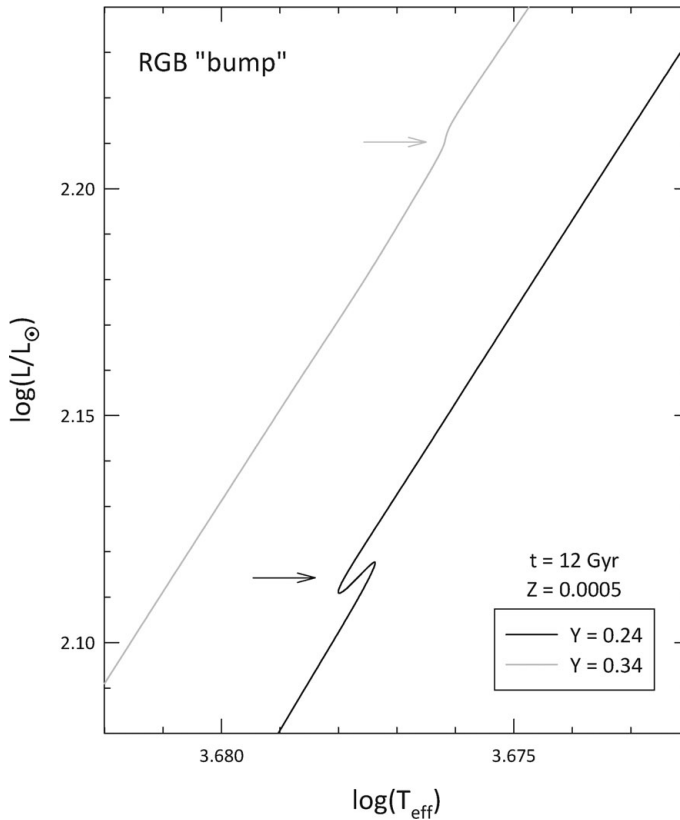


Figure 3. As Figure 1, but zooming in around the RGB-bump region.

noting that NGC 6441's 'twin,' NGC 6388, appears entirely consistent with the expectations for a 'normal' Y . Interestingly, Bono *et al.* also call attention to a possible increase in Y in the blue-HB cluster M13 (NGC 6205), but the measurements for this cluster are still consistent with a 'normal' Y , within the error bars.

RGB tip. As is clear from Figure 4, the luminosity of the RGB tip, where He ignition occurs, also depends on the He abundance, by an amount that is slightly less than 50% of that seen (at a fixed T_{eff}) on the MS. Therefore, GCs that lack first-generation stars and possess only second- and third-generation stars, as has been suggested for GCs with completely blue HBs (e.g., D'Antona & Caloi 2008), should have fainter RGB tips, by of order 0.11 mag for a difference in Y of 0.1 (Table 3). While evolution close to the RGB tip is quite fast, and therefore not many stars are usually found in that region of the CMD (which, in addition, may also contain AGB stars), careful analysis based on large samples might give indications of whether fainter RGB tips indeed tend to be more common, statistically speaking, in blue-HB GCs. In this sense, some authors have used the RGB-tip luminosity to place constraints on the He core mass at the He flash, M_c^{HeF} , which is of strong interest for particle physicists in particular. However, such studies have so far revealed evidence for large increases in neither M_c^{HeF} nor Y with respect to canonical values. On the contrary, available analyses have tended to favor a somewhat low He abundance see, e.g., figure 2 in Raffelt; and references therein), even though more detailed analysis of individual clusters, which has not been the focus of most such studies, would certainly prove of interest.

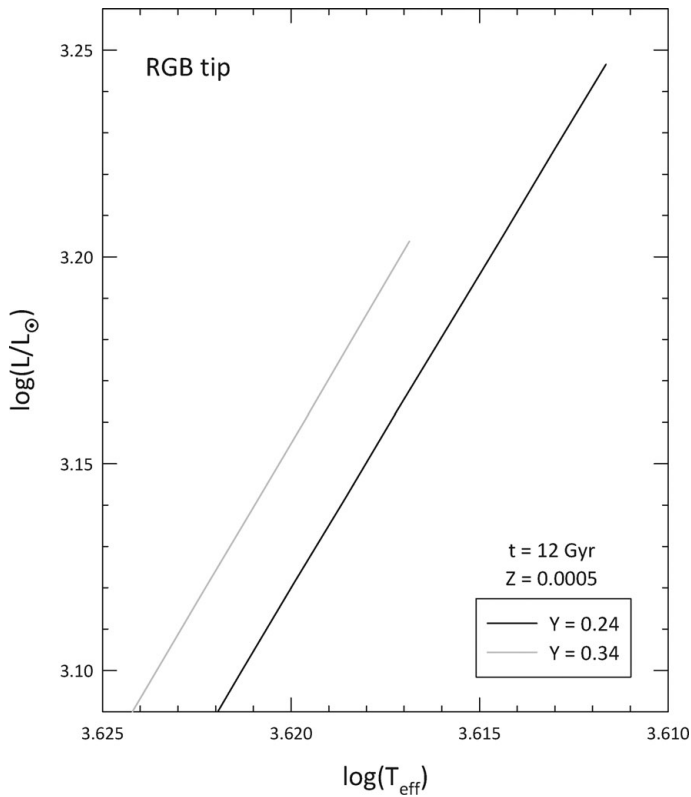


Figure 4. As Figure 1, but zooming in around the RGB-tip region.

As we have seen, contrary to the RGB tip, the RGB bump becomes *more* luminous with an increase in Y . Therefore, the difference in magnitude between the RGB tip and the RGB bump should be more sensitive to Y than either of these features alone. Based on Tables 1 and 2, we find $d\Delta M_{\text{bol}}(\text{RGB bump} - \text{tip})/dY = -3.6$, which is a stronger Y dependence than for many of the individual indicators listed in Table 4.

ZAHB. As well known, the ZAHB luminosity is strongly sensitive to Y (see, e.g., Sweigart 1987; and also our Figures 1, 5 and 6). This strong dependence constitutes the basis for a number of methods that are often used to infer the He abundance in GCs.

One such method is the ‘ A method’ of Caputo & Castellani (1975), which uses the fact that the periods of RR Lyrae stars depend strongly on their luminosities, and the latter on Y , to infer the He abundance on the basis of period and temperature measurements for RR Lyrae variables. Related to this are the so-called ‘period-shift techniques,’ in which differences in period, at a given temperature, are taken as evidence for variations in luminosity, and hence Y . Based on these techniques, an overluminosity, and hence evidence for an increase in Y , could not be detected among either ω Cen’s (Sollima *et al.* 2006) or NGC 1851’s (Lee *et al.* 2009) RR Lyrae stars. Similarly, Sandquist (2000) could not confirm the presence of significant He-abundance variations in his analysis of a large number of GCs, although he found a difference between metal-poor and moderately metal-rich objects, concluding however that “it is unlikely that the difference in $\langle A \rangle$ between the two groups is due to a difference in helium abundance.” On the other hand, large overluminosities, possibly related to He enhancement, have been confirmed for the metal-rich bulge GCs NGC 6388 and NGC 6441, which are known to contain large

Table 1. Evolutionary predictions for $Y = 0.24$.^a

Stage	M/M_{\odot}	$\log T_{\text{eff}}$	$\log(L/L_{\odot})$
MS ^b	0.606	3.699	-0.744
MS ^c	0.661	3.738	-0.500
TO	0.815	3.815	0.379
SGB ^d	0.832	3.785	0.622
SGB ^e	0.833	3.780	0.636
Base RGB ^f	0.838	3.725	0.879
Base RGB ^g	0.839	3.719	1.000
RGB bump	0.843	3.679	2.112
RGB tip	0.844	3.611	3.247
ZAHB ^h	0.663	3.850	1.650
AGB clump	0.663	3.708	2.012

NOTES:

^a For an assumed $Z = 0.0005$, $t = 12$ Gyr.

^b For a temperature $T_{\text{eff}} = 5000$ K.

^c For a luminosity $\log(L/L_{\odot}) = -0.50$.

^d At a temperature cooler than the TO by $\Delta \log T_{\text{eff}} = 0.03$.

^e At a temperature $\log T_{\text{eff}} = 3.780$.

^f At a level more luminous than the TO by $\Delta \log(L/L_{\odot}) = 0.5$.

^g At a luminosity $\log(L/L_{\odot}) = 1.0$.

^h At a temperature $\log T_{\text{eff}} = 3.850$.

Table 3. Differences between evolutionary predictions.^a

Stage	$\Delta(M/M_{\odot})$	$\Delta \log T_{\text{eff}}$	$\Delta \log(L/L_{\odot})$
MS ^b	-0.093	—	-0.105
MS ^c	-0.084	+0.016	—
TO	-0.128	+0.007	-0.058
SGB ^d	-0.133	+0.007	-0.033
SGB ^e	-0.133	—	-0.006
Base RGB ^f	-0.134	+0.012	-0.058
Base RGB ^g	-0.134	+0.008	—
RGB bump	-0.135	-0.003	+0.099
RGB tip	-0.136	+0.006	-0.044
ZAHB ^h	-0.038	—	+0.120
AGB clump	-0.038	+0.016	+0.145

NOTES:

^a In the sense $Y = 0.34$ minus $Y = 0.24$, for an assumed $Z = 0.0005$, $t = 12$ Gyr.

^b For a temperature $T_{\text{eff}} = 5000$ K.

^c For a luminosity $\log(L/L_{\odot}) = -0.50$.

^d At a temperature cooler than the TO by $\Delta \log T_{\text{eff}} = 0.03$.

^e At a temperature $\log T_{\text{eff}} = 3.780$.

^f At a level more luminous than the TO by $\Delta \log(L/L_{\odot}) = 0.5$.

^g At a luminosity $\log(L/L_{\odot}) = 1.0$.

^h At a temperature $\log T_{\text{eff}} = 3.850$.

Table 2. Evolutionary predictions for $Y = 0.34$.^a

Stage	M/M_{\odot}	$\log T_{\text{eff}}$	$\log(L/L_{\odot})$
MS ^b	0.513	3.699	-0.849
MS ^c	0.577	3.754	-0.500
TO	0.687	3.822	0.321
SGB ^d	0.699	3.792	0.591
SGB ^e	0.700	3.780	0.630
Base RGB ^f	0.704	3.737	0.821
Base RGB ^g	0.705	3.727	1.000
RGB bump	0.708	3.676	2.211
RGB tip	0.708	3.617	3.203
ZAHB ^h	0.625	3.850	1.770
AGB clump	0.625	3.724	2.157

NOTES:

^a For an assumed $Z = 0.0005$, $t = 12$ Gyr.

^b For a temperature $T_{\text{eff}} = 5000$ K.

^c For a luminosity $\log(L/L_{\odot}) = -0.50$.

^d At a temperature cooler than the TO by $\Delta \log T_{\text{eff}} = 0.03$.

^e At a temperature $\log T_{\text{eff}} = 3.780$.

^f At a level more luminous than the TO by $\Delta \log(L/L_{\odot}) = 0.5$.

^g At a luminosity $\log(L/L_{\odot}) = 1.0$.

^h At a temperature $\log T_{\text{eff}} = 3.850$.

Table 4. Predicted slopes.^a

Stage	$\frac{d \log T_{\text{eff}}}{dY}$	$\frac{d \log(L/L_{\odot})}{dY}$	$\frac{dM_{\text{bol}}}{dY}$
MS ^b	—	-1.05	+2.63
MS ^c	+0.16	—	—
TO	+0.07	-0.58	+1.45
SGB ^d	+0.07	-0.33	+0.83
SGB ^e	—	-0.06	+0.15
Base RGB ^f	+0.12	-0.06	+0.15
Base RGB ^g	+0.08	—	—
RGB bump	-0.03	+0.99	-2.48
RGB tip	+0.06	-0.44	+1.10
ZAHB ^h	—	+1.20	+3.00
AGB clump	+0.16	+1.45	+3.63

NOTES:

^a In the sense $Y = 0.34$ minus $Y = 0.24$, for an assumed $Z = 0.0005$, $t = 12$ Gyr.

^b For a temperature $T_{\text{eff}} = 5000$ K.

^c For a luminosity $\log(L/L_{\odot}) = -0.50$.

^d At a temperature cooler than the TO by $\Delta \log T_{\text{eff}} = 0.03$.

^e At a temperature $\log T_{\text{eff}} = 3.780$.

^f At a level more luminous than the TO by $\Delta \log(L/L_{\odot}) = 0.5$.

^g At a luminosity $\log(L/L_{\odot}) = 1.0$.

^h At a temperature $\log T_{\text{eff}} = 3.850$.

populations of RR Lyrae and blue HB stars, an uncommon feature in the metal-rich domain, which by itself may also point to the need for He enhancement (e.g., Sweigart & Catelan 1998; Pritzl *et al.* 2002; Caloi & D’Antona 2007; Busso *et al.* 2007).

Another method which exploits the strong dependence of HB luminosities on Y is the ‘ Δ method’ of Caputo *et al.* (1983), which uses the difference in magnitude between the HB and the MS as a He indicator. This is a particularly strong Y indicator because, while the HB luminosity increases with Y , the MS luminosity decreases. Based on Tables 1 and

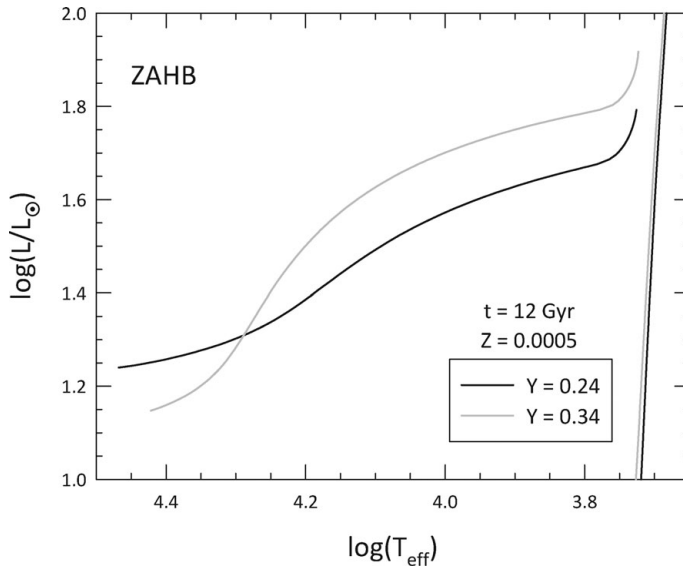


Figure 5. As Figure 1, but zooming in around the ZAHB region.

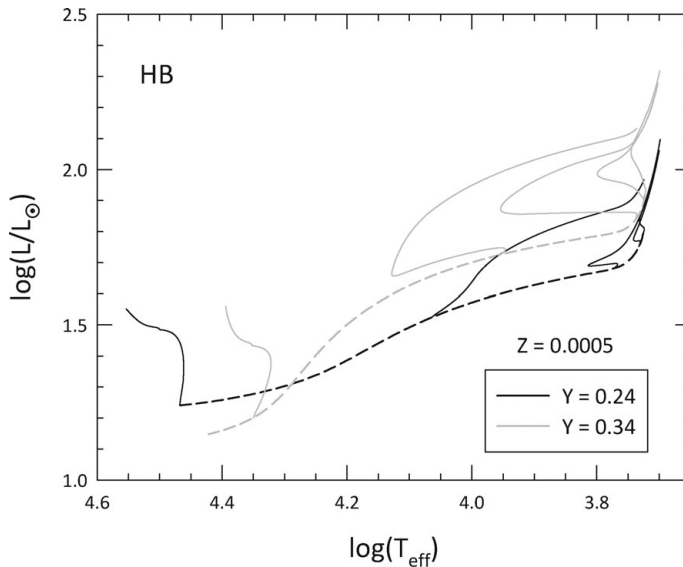


Figure 6. As Figure 5, but including evolutionary tracks for the following mass values (from left to right): 0.49, 0.60, 0.70, 0.80 and 0.90 M_{\odot} . The same ZAHB sequences as in the previous figure are shown as dashed lines.

2, we find $d\Delta M_{\text{bol}}(\text{MS} - \text{ZAHB})/dY = 5.6$. Sandquist (2000) applied this method to a large sample of GCs, but did not find evidence for significant variations in Y .

Finally, the increased luminosities of He-enhanced HB stars also lead to decreased surface gravities at a given T_{eff} . Therefore, and as suggested by several authors (see, e.g., Catelan 2009; and references therein), spectroscopic $\log g$ measurements can also be of interest in constraining the amount of He enhancement, particularly among blue-HB stars cooler than 11 500 K, whose atmospheres are not affected by the strong diffusion effects that make it extremely difficult to properly interpret the results for hotter HB

stars. In this sense, the method was recently applied to the GCs M3 (NGC 5272) and M13 by Catelan *et al.* (2009), but no evidence for an increase in Y over the canonical value was found for either cluster. In fact, these authors found, on the basis of a detailed analysis of Strömgren photometry for M3, that the amount of He enhancement among the cluster's blue-HB stars is likely less than 0.01 in Y , thus ruling out the much higher He enhancements that have been proposed in the literature.

HB. The color distribution of HB stars has been widely used in recent years to study the level of He enhancement in GCs (e.g., D'Antona & Caloi 2008; and references therein). The main reason why high- Y GCs of a given age and metallicity are expected to have a bluer HB morphology is the fact that their more compact progenitors evolve faster. Thus, at a given age, high- Y GCs feed stars of lower mass (and thus bluer; see Figure 6) onto the HB phase than their lower- Y counterparts. However, the colors of HB stars are sensitive not only to the He abundance, but also to many other parameters, such as age, CNO and α -element abundances, rotation and—crucially—mass loss on the RGB (see Catelan 2009 for a recent review). It is thus important to use indicators other than the color distribution of HB stars to establish whether, and to what level, He may be enhanced among HB stars. In this sense, the *luminosity distribution* of HB stars also plays a very important role that should not be ignored (e.g., Crocker *et al.* 1988; Fusi Pecci *et al.* 1996; Sweigart & Catelan 1998; Salaris *et al.* 2006, 2008; Catelan *et al.* 2009).

Examination of Figure 6 reveals that not only ZAHB luminosities (and their run with T_{eff}), but also other HB features, are sensitive to the He abundance. Note, in particular, that high- Y evolutionary tracks tend to evolve much more significantly in luminosity than at lower Y , which leads to an increase in the HB ‘thickness’ (or luminosity width) with increasing Y . Similarly, an increase in Y leads to much more pronounced ‘blueward loops,’ which also has important observational consequences (e.g., Sweigart & Catelan 1998; Pritzl *et al.* 2002; Catelan 2009). In addition, the predicted separation in luminosity between extreme-HB (EHB) stars and post-EHB stars is also a strong function of Y (Brown *et al.* 2008), which could, at least in principle, provide a test of He enhancement for those clusters for which extensive ultraviolet photometry is available.

Another key He abundance indicator for GCs that is based on properties of HB stars is the number ratio R of HB stars and RGB stars brighter than the HB (Iben 1968). In brief, not only does the HB luminosity increase markedly with increasing Y , but also HB lifetimes—and thus the number of HB stars relative to RGB stars brighter than the HB—increase markedly with increasing Y . Indeed, for HB stars beginning their evolution close to the instability strip, our models give $dR/dY = 8.3$,[†] thus confirming the strong sensitivity of the method to He-abundance variations.

The most recent application of this method to a large sample of GCs is the one by Salaris *et al.* (2004). They find that “the mean... $Y = 0.250 \pm 0.006$. An intrinsic dispersion with a firm upper limit of 0.019 around this value... is a priori possible given the observational errors.” Interestingly, the authors find some evidence for higher R values for clusters with blue HBs, as would be expected in the He-enhancement scenario. However, they point out that this result may be more straightforwardly explained in terms of an increase in HB lifetimes for bluer, less massive HB stars (see also Zoccali *et al.* 2000). **AGB clump.** According to our results (e.g., Table 3), the AGB clump, which is seen in some GCs at the base of the AGB, becomes significantly brighter with increasing Y . The

[†] This decreases to $dR/dY = 5.8$ if we assume that the HB luminosity taken as reference for RGB number counts is the same for both He-rich and He-poor models, as might be more appropriate for clusters for which stars on the ‘horizontal’ part of the HB are not He-enhanced, for which, in addition, one should consider that a fraction of the RGB stars might also be poor in He (see also Riello *et al.* 2003; Salaris *et al.* 2004).

difference in luminosity between the AGB clump and the ZAHB is, however, much less strongly dependent on Y , with $dM_{\text{bol}}(\text{ZAHB} - \text{AGB clump})/dY \approx 0.3$ (see also Bono *et al.* 1995). In addition, AGB clumps are only found in GCs with predominantly red HBs, which are not expected to be the ones displaying the largest levels of He enhancement.

3. Conclusions

Nature has conspired to make reliable measurements of the He abundance of GC stars an extremely difficult task. Still, many features of the CMD, besides MS and HB colors, present at least some sensitivity to Y . These can be best exploited, depending on the specific CMD location, in different wavelength regimes, using a variety of photometric and spectroscopic techniques. It is thus important to establish, on a cluster-by-cluster basis, which features are consistent (or not), to the limit of our empirical and theoretical knowledge, with the He-enhancement levels that have been suggested. Only then will we be in a good position to firmly establish the extent to which such He enhancements occur in nature. This is a crucial task to establish the role played by GCs as laboratories of stellar evolution and indeed, more generally, of astrophysics.

Acknowledgements

Support for M.C. is provided by Proyecto Basal PFB-06/2007, FONDAF Centro de Astrofísica 15010003, Proyecto FONDECYT Regular #1071002 and a John Simon Guggenheim Memorial Foundation Fellowship. Support for A.V. is provided by the IAU, CONICYT, SOCHIAS, MECESUP and ALMA.

References

- Behr, B. B. 2003, *ApJS*, 149, 67
- Bono, G., Cassisi, S., Zoccali, M., & Piotto, G. 2001, *ApJ* (Letters), 546, L109
- Bono, G., Castellani, V., Degl'Innocenti, S., & Pulone, L. 1995, *A&A*, 297, 115
- Brown, T. M., Smith, E., Ferguson, H. C., Sweigart, A. V., Kimble, R. A., & Bowers, C. W. 2008, *ApJ*, 682, 319
- Busso, G., *et al.* 2007, *A&A*, 474, 105
- Caloi, V. & D'Antona, F. 2005, *A&A*, 435, 987
- Caloi, V. & D'Antona, F. 2007, *A&A*, 463, 949
- Caputo, F. & Castellani, V. 1975, *Ap&SS*, 38, 39
- Caputo, F., Cayrel, R., & Cayrel de Strobel, G. 1983, *A&A*, 123, 135
- Carretta, E., Bragaglia, A., Gratton, R., & Lucatello, S. 2009, *A&A*, in press (arXiv:0909.2941)
- Carretta, E., *et al.* 2007, *A&A*, 464, 939
- Cassisi, S., Salaris, M., Anderson, J., Piotto, G., Pietrinferni, A., Milone, A., Bellini, A., & Bedin, L. R. 2009, *ApJ*, 702, 1530
- Cassisi, S., Salaris, M., Pietrinferni, A., Piotto, G., Milone, A. P., Bedin, L. R., & Anderson, J. 2008, *ApJ* (Letters), 672, L115
- Catelan, M. 2008, *MemSAIt*, 79, 388
- Catelan, M. 2009, *Ap&SS*, 320, 261
- Catelan, M., Grundahl, F., Sweigart, A. V., Valcarce, A. A. R., & Cortés, C. 2009, *ApJ* (Letters), 695, L97
- Crocker, D. A., Rood, R. T., & O'Connell, R. W. 1988, *ApJ*, 332, 236
- D'Antona, F., Bellazzini, M., Caloi, V., Fusi Pecci, F., Galletti, S., & Rood, R. T. 2005, *ApJ*, 631, 868
- D'Antona, F. & Caloi, V. 2008, *MNRAS*, 390, 693
- Davis, D. S., Richer, H. B., Anderson, J., Brewer, J., Hurley, J., Kalirai, J. S., Rich, R. M., & Stetson, P. B. 2008, *AJ*, 135, 2155

- Dupree, A. K., Smith, G. H., & Strader, J. 2009, *AJ*, 138, 1485
- Ferraro, F. R., Valenti, E., Straniero, O., & Origlia, L. 2006, *ApJ*, 642, 225
- Fusi Pecci, F., Bellazzini, M., Ferraro, F. R., Buonanno, R., & Corsi, C. E. 1996, in: H. Morrison & A. Sarajedini (eds.) *Formation of the Galactic Halo Inside and Out*, ASP Conf. Ser., Vol. 92, p. 221 (San Francisco: ASP)
- Girardi, L., Castelli, F., Bertelli, G., & Nasi, E. 2007, *A&A*, 468, 657
- Gratton, R. G., Carretta, E., Matteucci, F., & Sneden, C. 2000, *A&A*, 358, 671
- Grundahl, F., Catelan, M., Landsman, W. B., Stetson, P. B., & Andersen, M. I. 1999, *ApJ*, 524, 242
- Iben Jr., I. 1968, *Nature*, 220, 143
- Lee, J.-W., Lee, J., Kang, Y.-W., Lee, Y.-W., Han, S.-I., Joo, S.-J., Rey, S.-C., & Yong, D. 2009, *ApJ* (Letters), 695, L78
- Marcolini, A., Gibson, B. K., Karakas, A. I., & Sánchez-Blázquez, P. 2009, *MNRAS*, 395, 719
- Marino, A. F., Villanova, S., Piotto, G., Milone, A. P., Momany, Y., Bedin, L. R., & Medling, A. M. 2008, *A&A*, 490, 625
- Moehler, S. 2001, *PASP*, 113, 1162
- Moehler, S., Dreizler, S., Lanz, T., Bono, G., Sweigart, A. V., Calamida, A., Monelli, M., & Nonino, M. 2007, *A&A* (Letters), 475, L5
- Moehler, S., Landsman, W. B., Sweigart, A. V., & Grundahl, F. 2003, *A&A*, 405, 135
- Moehler, S., Sweigart, A. V., Landsman, W. B., & Dreizler, S. 2009, *Ap&SS*, 291, 231
- Norris, J. E. 2004, *ApJ* (Letters), 612, L25
- Palmieri, R., Piotto, G., Saviane, I., Girardi, L., & Castellani, V. 2002, *A&A*, 392, 115
- Pietrinferni, A., Cassisi, S., Salaris, M., Percival, S., & Ferguson, J. W. 2009, *ApJ*, 697, 275
- Piotto, G. 2009, *Proc. Int'l Astron. Union*, 4, 233
- Piotto, G., *et al.* 2005, *ApJ*, 621, 777
- Piotto, G., *et al.* 2007, *ApJ* (Letters), 661, L53
- Pritzl, B. J., Smith, H. A., Catelan, M., & Sweigart, A. V. 2002, *AJ*, 124, 949
- Raffelt, G. G. 1996, *Stars as Laboratories for Fundamental Physics: The Astrophysics of Neutrinos, Axions, and Other Weakly Interacting Particles* (Chicago: Univ. of Chicago Press)
- Raffelt, G. G. 2000, *Phys. Rep.*, 333, 593
- Raffelt, G. G. 2008, *Lect. Notes Phys.*, 741, 51
- Riello, M., *et al.* 2003, *A&A*, 410, 553
- Salaris, M., Cassisi, S., & Pietrinferni, A. 2008, *ApJ* (Letters), 678, L25
- Salaris, M., Chieffi, A., & Straniero, O. 1993, *ApJ*, 414, 580
- Salaris, M., Riello, M., Cassisi, S., & Piotto, G. 2004, *A&A*, 420, 911
- Salaris, M., Weiss, A., Ferguson, J. W., & Fusilier, D. J. 2006, *ApJ*, 645, 1131
- Sandquist, E. L. 2000, *MNRAS*, 313, 571
- Sollima, A., Borissova, J., Catelan, M., Smith, H. A., Minniti, D., Cacciari, C., & Ferraro, F. R. 2006, *ApJ* (Letters), 640, L43
- Sollima, A., Ferraro, F. R., Pancino, E., & Bellazzini, M. 2005, *MNRAS*, 357, 265
- Sweigart, A. V. 1987, *ApJS*, 65, 95
- Sweigart, A. V. & Catelan, M. 1998, *ApJ*, 501, L63
- Valcarce, A. A. R. 2010, Ph.D. Thesis, Pontificia Universidad Católica de Chile (in prep.)
- Ventura, P., Caloi, V., D'Antona, F., Ferguson, J., Milone, A., & Piotto, G. P. 2009, *MNRAS*, 399, 934
- Villanova, S., Piotto, G., & Gratton, R. 2009, *A&A*, 499, 755
- Yong, D., Grundahl, F., D'Antona, F., Karakas, A. I., Lattanzio, J. C., & Norris, J. E. 2009, *ApJ* (Letters), 695, L62
- Yong, D., Grundahl, F., Johnson, J. A., & Asplund, M. 2008, *ApJ*, 684, 1159
- Yoon, S.-J., Joo, S.-J., Ree, C. H., Han, S.-I., Kim, D.-G., & Lee, Y.-W. 2008, *ApJ*, 677, 1080
- Zoccali, M., Cassisi, S., Bono, G., Piotto, G., Rich, R. M., & Djorgovski, S. G. 2000, *ApJ*, 538, 289